Double-diffusive Hadley-Prats flow in a horizontal porous layer with a concentration based internal heat source

Anjanna Matta [a], P. A. L. Narayana [a], A. A. Hill [b,*]

[a] *Department of Mathematics, Indian Institute of Technology Hyderabad, Hyderabad - 502285, Telangana, India*

[b] *Department of Mathematical Sciences, University of the West England, Bristol, UK*

Abstract

Double-diffusive Hadley-Prats flow with a concentration based heat source is investigated through linear and non-linear stability analyses. The resultant eigenvalue problems for both theories are solved numerically using Shooting and fourth order Runga-Kutta methods, with the critical thermal Rayleigh number being evaluated with respect to various flow governing parameters such as the magnitudes of the heat source and mass flow. It is observed, in the linear case, that an increase in the horizontal thermal Rayleigh number is stabilising for both positive and negative values of the solutal Rayleigh number. In non-linear case, a destabilizing effect is identified at higher mass flow rates. An increase in both the heat source and mass flow results in destabilisation.

Key words: Double diffusive convection, porous medium, heat source, mass flow, Energy stability analysis.

1 Introduction

Double-diffusive convection in a fluid-saturated porous media has received much attention during the last few decades, due to its many real-world applications such as underground energy transport (Nagano et al. [1]), food processing, oil recovery, the spreading of pollutants etc. (Bendrichi and Shemilt [2]; Reddy et al. [3]) and multiple

* Corresponding author.
Email addresses: anjireddyiitm@gmail.com (Anjanna Matta), ananth@iith.ac.in (P. A. L. Narayana), antony.hill@uwe.ac.uk (A. A. Hill).

environmental processes (Xi and Li[4] and Kwon et al. [5]). A collection of comprehensive theories and experiments on double diffusive convection in porous media are presented in Ingham and Pop [6], Vafai [7], Nield and Bejan [8].

Of particular interest to the present study are investigations focusing on the phenomenon of double-diffusive convection in a shallow horizontal layer of a porous medium subject to inclined thermal and solutal gradients at both walls. Concerning the mono-diffusive case, non-homogeneity on the temperature conditions at both walls induces a basic flow (Hadley flow), which was first studied by Weber [13], and extended by Nield [14]. Nield et al. [15] further studied double diffusive Hadley flow due to inclined thermal and solutal gradients in a fluid saturated horizontal porous medium. An extension of this work with horizontal mass flow is due to Manole et al. [16]. If the flow is subjected to horizontal mass flow along with inclined thermal gradients, the resultant flow is known as Hadley-Prats flow (Barletta and Nield [17]). All the aforementioned works are related to linear stability analysis, to determine the critical values of the problem parameters and the nature of the instability in a well packed, low permeability porous media, so that the flow in the porous medium can be represented by Darcy flow model.

In the Lyapunov sense, linear stability theory gives sufficient conditions for instability, where the disturbance of the basic flow is unstable, whereas non-linear theory provides a sufficient condition for the disturbance to be asymptotically stable. Several problems in non-linear stability analysis using energy method are discussed by Kaloni and his contributors (Guo and Kaloni [9]; Kaloni and Qiao [10]; Kaloni and Qiao [11]). A collection of available studies for non-linear theory is given by Straughan [12]. The development of both linear instability and energy stability theories allows for the assessment of potential regions of subcritical instabilities in which convection could commence before the linear instability threshold is reached.

The motivation of the present work is to investigate double-diffusive Hadley flow in porous media induced by the active absorption of radiation, as demonstrated by

Krishnamurti [18] for a viscous fluid in the absence of Hadely circulation and Hill [19] for flows through porous media. Their model has received much attention in recent years as it provides an accurate model of cumulus convection as it occurs in the atmosphere. In addition to exploring a linear theory for the double-diffusive Hadley-Prats flow with concentration based internal heat source, we develop a complementary energy theory. The use of energy theory is the context of double-diffusive convection has been utilised extensively including Carr [20], Guo and Kaloni [9] and Hill [19]. We organize the paper in the following manner: section 2 constructs the governing equations of the model under consideration; in sections 3 & 4 we discuss the basic-state solution and perturbation equations; in sections 5 & 6 linear and non-linear analyses are performed, respectively, with the results and conclusions being discussed in sections 7 and 8, respectively.

2 Governing Equations

An infinite shallow horizontal fluid saturated porous layer with height d, confined between two isothermal and isosolutal fixed plates with concentration based internal heat source Q^* is considered. The Cartesian coordinates are chosen such that the z^*-axis is vertically upwards and there is a net flow along the direction of x^*-axis with magnitude u_0 as given in Fig. 1. A uniform concentration difference ∇S and a temperature difference $\nabla\theta$ are maintained between the lower and upper plates. Flow in the porous medium is governed by the Darcy law and the Oberbeck-Boussinesq approximation is invoked (such that the density variations are assumed to be sufficiently small to be neglected everywhere except in the body force term), and density ρ_f^* of the fluid is given by

$$\rho_f^* = \rho_0 \left[1 - \gamma_S \left(S^* - S_0\right) - \gamma_\theta \left(\theta^* - \theta_0\right)\right],$$

where S^* is the concentration, θ^* is the temperature, γ_S and γ_θ are the volumetric solutal and thermal expansion coefficients in the porous medium, and ρ_0 is the density at concentration S_0 and temperature θ_0. The governing system is given by the Darcy velocity in porous media, the concentration equation and the temperature equation such that

$$\nabla^{*}\cdot q^{*}=0\ , \tag{1}$$

$$\frac{\mu}{K}q^{*}+\nabla^{*}P^{*}-\rho_{f}^{*}g_{0}\mathbf{k}=0, \tag{2}$$

$$\phi\left(\frac{\partial S^{*}}{\partial t^{*}}\right)+q^{*}\cdot\nabla^{*}S^{*}=D_{m}\nabla^{*^{2}}S^{*} \tag{3}$$

$$(\rho c)_{m}\left(\frac{\partial\theta^{*}}{\partial t^{*}}\right)+(\rho c_{p})_{f}\,q^{*}\cdot\nabla^{*}\theta^{*}=k_{m}\nabla^{*^{2}}\theta^{*}+Q^{*}\left(S^{*}-S_{0}\right), \tag{4}$$

where Eq. (1) is the incompressibility condition. The boundary conditions are given by

$$z^{*}=-\frac{1}{2}d:\quad w^{*}=0,\quad S^{*}=S_{0}+\frac{\triangle S}{2}-\beta_{S_{x}}x^{*}-\beta_{S_{y}}y^{*},\quad \theta^{*}=\theta_{0}+\frac{\triangle\theta}{2}-\beta_{\theta_{x}}x^{*}-\beta_{\theta_{y}}y^{*},$$

$$z^{*}=\frac{1}{2}d:\quad w^{*}=0,\quad S^{*}=S_{0}-\frac{\triangle S}{2}-\beta_{S_{x}}x^{*}-\beta_{S_{y}}y^{*},\quad \theta^{*}=\theta_{0}-\frac{\triangle\theta}{2}-\beta_{\theta_{x}}x^{*}-\beta_{\theta_{y}}y^{*}. \tag{5}$$

Here $q^{*}=(u^{*},v^{*},w^{*})$ is the velocity, P^{*} is the pressure, μ is the viscosity, D_m is the solutal diffusivity, k_m is the thermal conductivity, g_0 is the gravity acceleration and $\mathbf{k}$ is the unit vector in the z^{*}-direction. The imposed horizontal components of solutal and thermal gradients to be $(\beta_{S_x},\ \beta_{S_y})$ and $(\beta_{\theta_x},\ \beta_{\theta_y})$, respectively. K and ϕ are the permeability and porosity of the medium, respectively. The subscripts f and m refer to the fluid and porous medium, respectively. c_p and c are the specific heats of the fluid and solid components. Here $(\rho c_p)_f$ and $(\rho c)_m$ are volumetric heat capacities for the fluid and solid phases. Following the scaling of Weber [13] and Nield [14], we define

$$x=\frac{x^{*}}{d},\quad y=\frac{y^{*}}{d},\quad z=\frac{z^{*}}{d},\quad t=\frac{\alpha_{m}t^{*}}{ad^{2}},\quad q=\frac{dq^{*}}{\alpha_{m}},\quad P=\frac{K\left(P^{*}+\rho_{0}g_{0}z^{*}\right)}{\mu\alpha_{m}},$$

$$\theta=\frac{R_{z}\left(\theta^{*}-\theta_{0}\right)}{\triangle\theta},\quad S=\frac{S_{z}\left(S^{*}-S_{0}\right)}{\triangle S},\quad Q=\frac{Q^{*}d^{2}R_{z}\triangle S}{k_{m}S_{z}\triangle\theta} \tag{6}$$

where

$$\alpha_{m}=\frac{k_{m}}{(\rho c_{p})_{f}},\quad a=\frac{(\rho c)_{m}}{(\rho c_{p})_{f}},\quad S_{z}=\frac{\rho_{0}g_{0}\gamma_{S}Kd\triangle S}{\mu D_{m}},\quad R_{z}=\frac{\rho_{0}g_{0}\gamma_{\theta}Kd\triangle\theta}{\mu\alpha_{m}}. \tag{7}$$

Here, S_z and R_z denote the vertical solutal and thermal Rayleigh numbers, respectively. The horizontal solutal and thermal Rayleigh numbers are defined as follows

$$S_x = \frac{\rho_0 g_0 \gamma_S K d^2 \beta_{S_x}}{\mu D_m}, \quad S_y = \frac{\rho_0 g_0 \gamma_S K d^2 \beta_{S_y}}{\mu D_m},$$

$$R_x = \frac{\rho_0 g_0 \gamma_\theta K d^2 \beta_{\theta_x}}{\mu \alpha_m}, \quad R_y = \frac{\rho_0 g_0 \gamma_\theta K d^2 \beta_{\theta_y}}{\mu \alpha_m}, \tag{8}$$

with $Le = \frac{\alpha_m}{D_m}$ being Lewis number and the non-dimensional net flow along the horizontal direction is defined as the Peclet number $M = \frac{u_0 d}{\alpha_m}$. Under these dimensionless variables, the governing Eqs. (1) - (4) take the following non-dimensional form

$$\nabla \cdot q = 0 \,, \tag{9}$$

$$q + \nabla P - \left(\frac{1}{Le} S + \theta \right) \mathbf{k} = 0, \tag{10}$$

$$\left(\frac{\phi}{a} \right) \frac{\partial S}{\partial t} + q \cdot \nabla S = \frac{1}{Le} \nabla^2 S, \tag{11}$$

$$\frac{\partial \theta}{\partial t} + q \cdot \nabla \theta = \nabla^2 \theta + QS, \tag{12}$$

with boundary conditions

$$z = -\frac{1}{2}: \quad w = 0, \quad S = \frac{S_z}{2} - S_x x - S_y y, \quad \theta = \frac{R_z}{2} - R_x x - R_y y,$$

$$z = \frac{1}{2}: \quad w = 0, \quad S = -\frac{S_z}{2} - S_x x - S_y y, \quad \theta = -\frac{R_z}{2} - R_x x - R_y y. \tag{13}$$

From Eqs. (9) - (12) we observe that all of the solutal and thermal Rayleigh numbers appear in the boundary conditions (13).

3 Steady-State Solution

Governing equations (9)-(12), subject to boundary conditions (13) admit a basic state solution of the form

$$S_s = \widetilde{S}(z) - S_x x - S_y y, \quad \theta_s = \widetilde{\theta}(z) - R_x x - R_y y,$$

$$u_s = u(z)\,, \quad v_s = v(z)\,, \quad w_s = 0, \quad P_s = P(x, y, z)\,, \tag{14}$$

where

$$u = -\frac{\partial P}{\partial x}, \quad v = -\frac{\partial P}{\partial y},$$

$$0 = -\frac{\partial P}{\partial z} + \left[\frac{1}{Le}\left(\widetilde{S}\,(z) - S_x x - S_y y\right) + \widetilde{\theta}\,(z) - R_x x - R_y y\right],$$

$$\frac{1}{Le} D^2 \widetilde{S} = -u S_x - v S_y, \quad D^2 \widetilde{\theta} + QS = -u R_x - v R_y. \tag{15}$$

Here $D = \frac{d}{dz}$ and $M = \int_{-1/2}^{1/2} u(z)\, dz$ is the net flow in the horizontal direction and $\int_{-1/2}^{1/2} v(z)\, dz = 0$. Peclet number M gives the strength of flow along the horizontal direction. We obtain the basic state solution in the form of flow velocity, concentration and temperature in the medium such that

$$u_s = \left(\frac{S_x}{Le} + R_x\right) z + M, \quad v_s = \left(\frac{S_y}{Le} + R_y\right) z, \quad w_s = 0, \tag{16}$$

$$\widetilde{S} = -S_z z + A, \quad \widetilde{\theta} = -R_z z + B, \tag{17}$$

where A, B, λ_1 and λ_2 are given by

$$A = \frac{\lambda_1}{24}\left(z - 4z^3\right) + \frac{M S_x Le}{8}\left(1 - 4z^2\right),$$

$$B = \frac{(\lambda_2 - Q S_z)}{24}\left(z - 4z^3\right) - \frac{M R_x}{8}\left(4z^2 - 1\right) + \frac{\lambda_1 Q}{24}\left(z^5/5 - z^3/6 + 7z/240\right) - \frac{Q M Le S_x}{8}\left(z^2/2 - z^4/3\right) + \frac{5 M S_x Le Q}{384},$$

$$\lambda_1 = {S_x}^2 + {S_y}^2 + Le\left(R_x S_x + R_y S_y\right), \quad \lambda_2 = {R_x}^2 + {R_y}^2 + \frac{R_x S_x + R_y S_y}{Le}. \tag{18}$$

The flow given by Eq. (16) is referred to as the Hadley-Prats flow.

4 Perturbation Equations

Introducing a perturbation of the form $q = q_s + q'$, $S = S_s + S'$, $\theta = \theta_s + \theta'$ and $P = P_s + P'$, and substituting these perturbations into the dimensionless governing equations (9) - (12) yields

$$\nabla \cdot q' = 0\,, \tag{19}$$

$$q' = -\nabla P' + \left(\frac{S'}{Le} + \theta'\right) \mathbf{k}, \tag{20}$$

$$\left(\frac{\phi}{a}\right)\frac{\partial S^{'}}{\partial t} + q_s\cdot\nabla S^{'} + q^{'}\cdot\nabla S_s + q^{'}\cdot\nabla S^{'} = \frac{1}{Le}\nabla^2 S^{'}, \tag{21}$$

$$\frac{\partial \theta^{'}}{\partial t} + q_s\cdot\nabla\theta^{'} + q^{'}\cdot\nabla\theta_s + q^{'}\cdot\nabla\theta^{'} = \nabla^2\theta^{'} + QS^{'}, \tag{22}$$

where

$$\nabla S_s = -\left(S_x, S_y, S_z - \widetilde{A}\right), \quad \nabla\theta_s = -\left(R_x, R_y, R_z - \widetilde{B}\right),$$

$$\widetilde{A} = \frac{\lambda_1}{24}\left[1 - 12z^2\right] - MS_xLez,$$

$$\widetilde{B} = \frac{(\lambda_2 - QS_z)}{24}\left(1 - 12z^2\right) + \frac{\lambda_1 Q}{24}\left(z^4 - \frac{z^2}{2} + \frac{7}{240}\right) - \frac{QMLeS_x}{24}\left(3z - 4z^3\right) - MR_xz\ .$$

The boundary conditions are

$$w^{'} = 0, \quad S^{'} = 0 \quad \theta^{'} = 0, \quad \text{at} \quad z = \pm\frac{1}{2}, \tag{23}$$

which state that there is zero perturbation in velocity, concentration and temperature at the upper and lower plates.

5 Linear Stability Analysis

The linearized perturbation equations are derived by neglecting the products of disturbances from Eqs. (19) - (22), yielding

$$\nabla\cdot q^{'} = 0\ , \tag{24}$$

$$q^{'} = -\nabla P^{'} + \left(\frac{S^{'}}{Le} + \theta^{'}\right)\mathbf{k}, \tag{25}$$

$$\left(\frac{\phi}{a}\right)\frac{\partial S^{'}}{\partial t} + u_s\frac{\partial S^{'}}{\partial x} + v_s\frac{\partial S^{'}}{\partial y} - S_xu^{'} - S_yv^{'} + \left(D\widetilde{S}\right)w^{'} = \frac{1}{Le}\nabla^2 S^{'}, \tag{26}$$

$$\frac{\partial \theta^{'}}{\partial t} + u_s\frac{\partial \theta^{'}}{\partial x} + v_s\frac{\partial \theta^{'}}{\partial y} - R_xu^{'} - R_yv^{'} + \left(D\widetilde{\theta}\right)w^{'} = \nabla^2\theta^{'} + QS^{'}, \tag{27}$$

where

$$D\widetilde{S} = -S_z + \frac{\lambda_1}{24}\left[1 - 12z^2\right] - MS_xLez,$$

$$D\widetilde{\theta} = -R_z + \frac{(\lambda_2 - QS_z)}{24}\left(1 - 12z^2\right) + \frac{\lambda_1 Q}{24}\left(z^4 - \frac{z^2}{2} + \frac{7}{240}\right) - \frac{QMLeS_x}{24}\left(3z - 4z^3\right) - MR_xz\ . \tag{28}$$

Since the resulting system is linear and autonomous, we may seek solutions of the normal modes form

$$\left[q^{'}, S^{'}, \theta^{'}, P^{'}\right] = \left[q\left(z\right), S\left(z\right), \theta\left(z\right), P\left(z\right)\right] \exp\left\{i\left(kx + ly - \sigma t\right)\right\} \tag{29}$$

and eliminate P from Eq. (25), to give

$$\left(D^2 - \alpha^2\right) w + \left(\frac{S}{Le} + \theta\right) \alpha^2 = 0, \tag{30}$$

$$\left(\frac{1}{Le}\left[D^2 - \alpha^2\right] + i\frac{\phi}{a}\sigma - iku_s - ilv_s\right) S + i\frac{1}{\alpha^2}\left(kS_x + lS_y\right) Dw - \left(D\widetilde{S}\right) w = 0, \tag{31}$$

$$\left(D^2 - \alpha^2 + i\sigma - iku_s - ilv_s\right) \theta + \frac{i}{\alpha^2}\left(kR_x + lR_y\right) Dw - \left(D\widetilde{\theta}\right) w + QS = 0, \tag{32}$$

where $i = \sqrt{-1}$ and $\alpha = \sqrt{k^2 + l^2}$ is the overall wave number. Equations (30) - (32) are subject to $w = S = \theta = 0$ at both the plates $z = \pm\frac{1}{2}$ and constitute an eigenvalue problem for vertical thermal Rayleigh number R_z with α, ϕ, Le, S_x, S_y, S_z, R_x, R_y, σ, k and l as parameters. The critical value of R_z is located by minimising over α. The term longitudinal disturbances are characterized by $k = 0$. Similarly, transverse disturbances are characterized by $l = 0$. Critical thermal Rayleigh number for the linear theory is given as $R_z = \min_\alpha R_z$. Numerical results for the linear theory are presented in section 7.

6 Non-Linear Stability Analysis

To obtain global non-linear stability bounds we multiply equations (20), (21) and (22) by $q^{'}$, $\beta^{'}$ and $\theta^{'}$, respectively, and integrate over the periodicity cell, denoted by Ω, which yields

$$||q^{'}||^2 = \langle\theta^{'} w^{'}\rangle + \langle\beta^{'} w^{'}\rangle, \tag{33}$$

$$\frac{L_e\phi}{2a}\frac{d||\beta^{'}||^2}{dt} = -\langle\left(q^{'}\cdot\nabla S_s\right)\beta^{'}\rangle - ||\nabla\beta^{'}||^2, \tag{34}$$

$$\frac{1}{2}\frac{d||\theta^{'}||^2}{dt} = -\langle\left(q^{'}\cdot\nabla\theta_s\right)\theta^{'}\rangle - ||\nabla\theta^{'}||^2 + QLe\langle\beta^{'}\theta^{'}\rangle, \tag{35}$$

where $\beta^{'} = \frac{S^{'}}{L_e}$, and $\langle \cdot \rangle$ denotes the integration over Ω and $|| \cdot ||$ represents $L^2(\Omega)$ norm. We obtain the following energy functional from Straughan [12]

$$E\left(t\right) = \frac{\xi}{2} \parallel \theta^{'} \parallel^2 + \frac{\eta L_e \phi}{2a} \parallel \beta^{'} \parallel^2 \tag{36}$$

where $\xi > 0$ and $\eta > 0$ are coupling parameters. Eqs. (33) - (35) and Eq. (36) can be put in the form

$$\frac{dE}{dt} = \mathcal{I} - \mathcal{D}, \tag{37}$$

where

$$\mathcal{I} = -\xi \langle \left(q^{'} \cdot \nabla \theta_s \right) \theta^{'} \rangle - \eta \langle \left(q^{'} \cdot \nabla S_s \right) \beta^{'} \rangle + \langle \theta^{'} w^{'} \rangle + \langle \beta^{'} w^{'} \rangle + \xi LeQ \langle \beta^{'} \theta^{'} \rangle, \tag{38}$$

$$\mathcal{D} = \eta ||\nabla \beta^{'}||^2 + \xi ||\nabla \theta^{'}||^2 + ||q^{'}||^2. \tag{39}$$

Defining

$$R_E = \max_{\mathcal{H}} \left(\frac{\mathcal{I}}{\mathcal{D}} \right) \tag{40}$$

where $\mathcal{H}$ is the space of all admissible solutions to equations (19) - (22), we have

$$\frac{dE}{dt} \leq -\mathcal{D} \left(1 - R_E\right). \tag{41}$$

The classical Poincaré inequality $||q^{'} - q^{'}_{\Omega}||_{L^p(\Omega)} \leq C ||\nabla q^{'}||_{L^p(\Omega)}$, where Ω is a open connected locally compact Hausdorff space and use of $q^{'}_{\Omega} = \frac{1}{|\Omega|} \int_{\Omega} q^{'} \left(y\right) dy$ yields

$$\frac{dE}{dt} \leq -2\pi^2 \left(1 - R_E\right) \min\{1, \frac{a}{L_e \phi}\} E. \tag{42}$$

The inequality (42) guarantees that $E\left(t\right) \to 0$ at least exponentially as $t \to \infty$ for $R_E < 1$. Since $E(t)$ does not contain the kinetic energy term for the velocity $||q^{'}||^2$, we apply the arithmetic-geometric mean inequality to Eq. (33) to yield

$$||q^{'}||^2 \leq 2 \left((||\beta^{'}||^2 + ||\theta^{'}||^2 \right). \tag{43}$$

From Eqs. (43) and (36) observed that the decay of $||q^{'}||$ is implied by the decay of $E\left(t\right)$ and hence the system is stable for $R_E < 1$. The corresponding Euler-Lagrange system for R_E is

$$\xi\theta^{'}\nabla\theta_s + \eta\beta^{'}\nabla S_s - \left(\theta^{'} + \beta^{'}\right)\mathbf{k} + 2R_E q^{'} = \nabla\pi^{'}, \tag{44}$$

$$w^{'} - \eta q^{'}\cdot\nabla S_s + LeQ\xi\theta^{'} + 2R_E\eta\nabla^2\beta^{'} = 0, \tag{45}$$

$$w' - \xi q^{'}\cdot\nabla\theta_s + Q\xi\beta^{'}z + 2R_E\xi\nabla^2\theta^{'} = 0. \tag{46}$$

Here $\pi^{'}$ is Lagrange multiplier introduced because $q^{'}$ is divergence free. While deriving the Eqs. (44) - (46), we let $\chi = (q^{'}, \beta^{'}, \theta^{'})$ and $L = \mathcal{I} - R_E\mathcal{D}$. Then the corresponding Euler-Lagrange system can be written as

$$\nabla_{\chi_i}L - \frac{\partial}{\partial x_j}\nabla_{\chi_i^\circ}L = 0 \quad \text{for} \quad i = 1,2,3; \quad j = 1,2,3$$

where $'\circ'$ denotes the differentiation with respect to z. We consider R_z as the eigenvalue and estimate the maximum variation of R_z with optimal choice of η and ξ. From Eqs. (44) - (46) we can derive

$$\frac{\partial R_z}{\partial\eta} = \frac{2\left(1+\xi R_z\right)\left[R_E\left(1-\eta S_z\right)||\nabla\beta^{'}||^2 + LeQ\xi S_z\langle\theta^{'}\beta^{'}\rangle + \langle\widetilde{A}\beta^{'}w^{'}\rangle - \Psi_S\right]}{\xi^2\left(1+\eta S_z\right)\left(2R_E||\nabla\theta^{'}||^2 + \langle\widetilde{B}\theta^{'}w^{'}\rangle - LeQ\langle\theta^{'}\beta^{'}\rangle - \Psi_R\right)}, \tag{47}$$

$$\frac{\partial R_z}{\partial\xi} = \frac{R_E\left(1-\xi R_z\right)||\nabla\theta^{'}||^2 + LeQ\xi R_z\langle\theta^{'}\beta^{'}\rangle + \langle\widetilde{B}\theta^{'}w^{'}\rangle - \Psi_R}{\xi^2\left(2R_E||\nabla\theta^{'}||^2 + \langle\widetilde{B}\theta^{'}w^{'}\rangle - LeQ\langle\theta^{'}\beta^{'}z\rangle - \Psi_R\right)}, \tag{48}$$

where

$$\Psi_S = S_x\langle\beta^{'}u^{'}\rangle + S_y\langle\beta^{'}v^{'}\rangle, \quad \Psi_R = R_x\langle\theta^{'}u^{'}\rangle + R_y\langle\theta^{'}v^{'}\rangle.$$

We also note that if $S_x = S_y = 0$, $R_x = R_y = 0$ and $Q = 0$, then

$$\frac{\partial R_z}{\partial\eta} = \frac{\left(1+\xi R_z\right)\left(1-\eta S_z\right)||\nabla\beta^{'}||^2}{\xi^2\left(1+\eta S_z\right)||\nabla\theta^{'}||^2}, \tag{49}$$

$$\frac{\partial R_z}{\partial\xi} = \frac{\left(1-\xi R_z\right)}{2\xi^2}, \tag{50}$$

which are also reported in Guo and Kaloni [9].

Equations (44) - (46) are solved for the cricial value $R_E = 1$. To evaluate this system numerically, we take the *curl curl* of Eq. (44) and further use the third component of the resulting equation, to find that

$$\begin{aligned}&\xi R_x\frac{\partial^2\theta'}{\partial x\partial z}+\xi R_y\frac{\partial^2\theta'}{\partial y\partial z}+\xi\nabla_1^2\left[\left(-R_z+\widetilde{B}\right)\theta'\right]+\eta S_x\frac{\partial^2\beta'}{\partial x\partial z}+\eta S_y\frac{\partial^2\beta'}{\partial y\partial z}+2\nabla_1^2w'\\&\quad+\eta\nabla_1^2\left[\left(-S_z+\widetilde{A}\right)\beta'\right]-\nabla_1^2\left(\theta'+\beta'\right)-2\left(\frac{\partial^2u'}{\partial x\partial z}+\frac{\partial^2v'}{\partial y\partial z}\right)=0,\end{aligned}\tag{51}$$

where $\nabla_1^2=\left(\frac{\partial^2}{\partial x^2}+\frac{\partial^2}{\partial y^2}\right)$. Applying normal modes

$$\left[q',\beta',\theta',\pi'\right]=\left[q\left(z\right),\beta\left(z\right),\theta\left(z\right),\pi\left(z\right)\right]\exp\left(i\left(kx+ly\right)\right),\tag{52}$$

with $(S_x,S_y)\cdot(k,l)=0$; $(R_x,R_y)\cdot(k,l)=0$, in Eqs. (44), (45), (46), (51) and eliminate u, v and π to obtain the following eigenvalue problem

$$D^2w=\alpha^2w+\alpha^2\eta h_1\beta+\alpha^2\xi h_2\theta,\tag{53}$$

$$D^2\beta=-h_1w+h_3\beta-\xi h_4\theta,\tag{54}$$

$$D^2\theta=h_2w-\eta h_4\beta+h_5\theta,\tag{55}$$

where

$$h_1=\frac{1}{2}\left[-S_z+\widetilde{A}-\eta^{-1}\right],\quad h_2=\frac{1}{2}\left[-R_z+\widetilde{B}-\xi^{-1}\right],\quad h_3=\alpha^2-\frac{\eta}{4}\left[S_x^2+S_y^2\right],$$

$$h_4=\frac{1}{4}\left[R_xS_x+R_yS_y+2LeQ\eta^{-1}\right],\quad h_5=\alpha^2-\frac{\xi}{4}\left[R_x^2+R_y^2\right],$$

and the corresponding boundary conditions are

$$w=\beta=\theta=0\ \text{ at }\ z=\pm\frac{1}{2}.\tag{56}$$

The critical vertical thermal Rayleigh number is obtained through

$$R_z=\max_{\xi}\max_{\eta}\min_{\alpha}R_z\left(\xi,\eta,\alpha,Q,M,Le,R_x,R_y,S_x,S_y,S_z\right).\tag{57}$$

Numerical comparison between the linear and non-linear theories are presented in the next section.

7 Results and Discussion

Our goal in this study is to bring out the effect of a concentration based heat source on the double-diffusive Hadley-Prats flow in porous media. We apply the numerical scheme which is proposed by Barletta and Nield [21] to solve the eigenvalue problem (30) - (32) for linear and (53) - (55) for non-linear cases, with respect to the boundary conditions (56), in which, we treat vertical thermal Rayleigh number (R_z) as the eigenvalue. Here, the critical R_z is defined as the minimum of all R_z values as α is varied in both linear and non-linear cases. In our computations, we consider both cases $S_z < 0$ and $S_z > 0$, where $S_z > 0$ represents the concentration on upper boundary being higher than that of lower boundary, with $S_z < 0$ being the reverse. In the present study, we set $\phi/a = 1$, $S_y = R_y = 0$ and $Le = 10$ as this is roughly representative of experiments with sugar or salt systems. Barletta and Nield [21] concluded for the Hadley-Prats flow, that the preferred mode of the disturbance is the non-oscillatory longitudinal mode. Hence, the results presented here are for $k = 0$ and $\sigma = 0$. In Table 1, the computation results of the critical values of R_z are illustrated for various values of S_z in the absence of horizontal Rayleigh numbers. In this table, R_{z_l} indicates critical R_z in linear case and R_{z_e} indicates the non-linear critical R_z. And also, α_l indicates the critical wave number in linear case and α_e indicates the critical wave number in non-linear case. From the Table 1, it is observed that when $R_x = R_y = S_x = S_y = 0$, $Q = 0$ and $M = 0$ the present results are in very good agreement with the existing results in the literature, due to Guo and Kaloni [9]. For an increase in the value of S_z from negative to positive, the critical value of R_z is reduced in the both linear and non-linear cases seen in Table 1. This indicates that the system becomes unstable as S_z increases.

In Figs. 2 to 7, we used fixed notation to represent linear and non-linear results. In these figures solid lines represent the linear stability results and the dashed lines represent the non-linear stability results.

The response of critical values of R_z as a function of horizontal mass flow M for both positive and negative values of S_z is shown in Figs. 2 and 3, respectively. In the absence of a heat source (Q), the linear results shows that increasing the mass flow in the medium destabilizes the convection. When Q is introduced, and for smaller values of M, the flow is initially stabilized, but once the magnitude of M takes higher values, this causes the destabilization of the flow seen in Figs. 2 and 3. Increasing the value of Q reduces the critical values of R_z with increasing mass flow in the linear case for $S_z > 0$ and $S_z < 0$. However, in the case of non-linear analysis, in the absence of Q, critical values of R_z are reduced with increasing the values of M, which is in contrast to the stabilization phenomenon observed in the linear case. From Fig. 3, when $S_z = -3$ and M increases, then the critical values of R_z decreases irrespective of heat source (Q) for both linear and non-linear cases. It means that the flow is destabilises as mass flow increases when $S_z = -3$. It is clearly observed that, when $Q = 0$ (i.e. there is no concentration based internal heat source) the difference between the linear and non-linear critical values increases with an increase in M, whereas, in the presence of a heat source ($Q > 0$), it is observed that this difference is reduced in Figs. 2 and 3. This indicates that, as the heat source increases, the sub-critical region is reduced. In all cases the critical value of R_z decreases with an increasing mass flow (M). This demonstrates that increasing the strength of M destabilises the system.

Figures 4 and 5 explore the variation of the critical values of R_z with horizontal temperature gradient R_x for positive and negative values of S_z, respectively, with different combinations of heat source (Q) and the horizontal mass flow (M). The linear theory demonstrates that an increase in the horizontal thermal Rayleigh number stabilizes the convection process, however introducing the mass flow in the critical values of R_z are reduced irrespective of heat source, hence for a fixed Q, mass flow causes stabilization in the linear case. Even for the non-linear case, in the absence or presence of the heat source and mass flow, increasing the R_x makes the flow more stable in Fig. 4. When S_z is negative from Fig. 5 it shows that the linear instability curves are similar to the linear observations made for positive S_z. However, this is contradicted in the non-linear results associated with positive S_z in the presence of M and Q at higher values of R_x. In this case, R_z decreases as a function of R_x with increasing mass flow in the medium, and also the flow is stabilised at higher values of R_x irrespective of Q and M seen in Fig. 5. The results indicate that both the linear and non-linear results undergo quantitative changes subject to horizontal thermal and solutal gradients along with the presence and absence of heat source and mass flow variations.

The response of critical values of R_z as a function of Le is visualized in Figs. 6 and 7 for positive and negative values of solutal Rayleigh number S_z, respectively, in the absence and presence of M at $Q = 0$. In the absence of horizontal mass flow (i.e. when $M = 0$) the critical value of R_z increases as Le increases and hence the flow become more stable. However, in the presence of M, the critical value of R_z is reduced by an increasing Le. The fall in the critical R_z in the non-linear theory is further enhanced by increasing Le as compared to linear theory when M is present seen for $S_z > 0$ and $S_z < 0$. The regions of potential sub-critical instability are small for $M = 0$ but increase substantially (as Le increases) in the presence of mass flow. In both cases for $S_z = 3$ and -3, the stability characteristics for linear and non-linear results differ considerably.

8 Conclusion

In the present article, we have explored the effect of concentration based heat source on the thermosolutal Hadley convection in porous media in the presence of mass flow, utilising linear and non-linear stability analysis. A comparison between the linear stability thresholds and energy stability thresholds is made by treating the vertical component of the thermal Rayleigh number as an eigenvalue. In both cases the vertical thermal Rayleigh number is evaluated for different combinations of the flow governing parameters. The results indicate the following conclusions:

- In the presence of a mass flow effect, the flow is destabilising in both the linear and non-linear cases.

- In the presence of a heat source and mass flow, the flow is stabilising at higher horizontal Rayleigh numbers in the linear case, whereas it is destabilizing in the non-linear case at larger mass flows.
- As the concentration based heat source increases, the sub-critical region increases.

References

[1] K. Nagano, T. Mochida, K. Ochifuji, Influence of natural convection on forced horizontal flow in saturated porous media for aquifer thermal energy storage, Applied Thermal Engineering, 12 (2002) 1299-1311.

[2] G. Bendrichi, L.W. Shemilt, Mass transfer in horizontal flow channels with thermal gradients, The Canadian Journal of Chemical Engineering 75 (1997) 1067-1074.

[3] K.S. Reddy, K.R. Kumar, C.S. Ajay, Experimental investigation of porous disc enhanced receiver for solar parabolic trough collector, Renewable Energy 77 (2015) 308-319.

[4] C. Xi , A. Li, An experimental study on particle deposition above near-wall heat source, Building and Environment 81 (2014) 139-149.

[5] O. Kwon, K. Bae, C. Park, Cooling characteristics of ground source heat pump with heat exchange methods, Renewable Energy 71 (2014) 651-657.

[6] D.B. Ingham, I. Pop, Transport phenomena in porous media. Oxford: Pergamon; 1998.

[7] K. Vafai Handbook of porous media. 2nd ed. Boca Raton: CRC Press; 2005.

[8] D.A. Nield, A. Bejan, Convection in Porous Media, forth ed., Springer 2013.

[9] J. Guo, P.N. Kaloni Nonlinear stability and convection induced by inclined thermal and solutal gradients. Z Angew Math Phys 46 (1995) 645-654

[10] P.N. Kaloni, Z. Qiao, Non-linear stability of convection in a porous medium with inclined temperature gradient, Int. J. Heat Mass Transfer 40 (1997) 1611-1615.

[11] P.N. Kaloni, Z. Qiao, Nonlinear convection induced by inclined thermal and solutal gradients with mass flow, Continuum Mech. Thermodyn. 12 (2000) 185-194.

[12] B. Straughan, The Energy Method, Stability, and nonlinear convection, second ed., Springer 2010.

[13] J.E. Weber, Convection in a porous medium with horizontal and vertical temperature gradients, Int. J. Heat Mass Transfer 17 (1974) 241-248.

[14] D.A. Nield, Convection in a porous medium with inclined temperature gradient and horizontal mass flow, Heat Transfer 5 (1990) 153-185.

[15] D.A. Nield, D.M. Manole and J.L. Lage, Convection induced by inclined thermal and solutal gradients in a shallow horizontal layer of a porous medium. J. Fluid Mech. 257 (1993) 559-574.

[16] D.M. Manole, J.L. Lage, D.A. Nield, Convection induced by inclined thermal and solutal gradients, with horizontal mass flow, in a shallow horizontal layer of a porous medium, Int. J. Heat Mass Transfer 37 (1994) 2047-2057.

[17] A. Barletta, D.A. Nield, Instability of Hadley-Prats Flow with Viscous Heating in a Horizontal Porous Layer,Transp. Porous Med. 84 (2010) 241-256.

[18] R. Krishnamurti, Convection induced by selective absorption of radiation: a laboratory model of conditional instability. Dynam. Atmos. Oceans 27 (1997) 367382.

[19] A.A. Hill, Double-diffusive convection in a porous medium with a concentration based internal heat source, Proc. R. Soc. A 461 (2005) 561-574.

[20] M. Carr, A model for convection in the evolution of under-ice melt ponds. Continuum Mech. Thermodyn. 15 (2003) 45-54.

[21] A. Barletta, D.A. Nield, On Hadley flow in a porous layer with vertical heterogeneity, J. Fluid Mech., vol. 710 (2012) 304-323. **30**, 21-31 (1967)

Nomenclature

d	height of porous layer
D_m	solutal diffusivity
g_0	acceleration due to gravity
K	permeability
k_m	thermal conductivity
Le	Lewis number
M	dimensionless mass flow
P	dimensionless pressure
R_x, R_y	horizontal thermal Rayleigh numbers
R_z	vertical thermal Rayleigh number
S_x, S_y	horizontal solutal Rayleigh numbers
S_z	vertical solutal Rayleigh number
q	dimensionless velocity
Q	dimensionless heat source
S	dimensionless concentration
t	dimensionless time
u, v, w	x, y, z component of dimensionless velocities

Greek symbols

α	dimensionless overall wave number
α_m	thermal diffusivity
$(\beta_{\theta_x}, \beta_{\theta_y})$	horizontal thermal gradient vector
$(\beta_{S_x}, \beta_{S_y})$	horizontal solutal gradient vector
γ_θ, γ_S	thermal and solutal expansion coefficients
θ	dimensionless temperature

ρ	density
Φ	porosity
ξ, η	coupling parameters

Subscripts

f	fluid region
m	porous medium
s	steady state

Superscripts

$*$	dimensional variables
$'$	disturbance quantities

S_z	-30	-20	-10	10^{-5}	10	20	30
R_{z_l}	69.478415	59.478415	49.478413	39.478301	29.478413	19.478414	9.478414
α_l	3.141600	3.141600	3.141600	3.141600	3.141600	3.141600	3.141600
R_{z_e}	39.478396	39.478396	39.478396	39.478308	29.478411	19.478411	9.478412
α_e	3.141600	3.141600	3.141600	3.141600	3.141600	3.141600	3.141600

Table 1
Linear and non-linear case critical thermal Rayleigh number for $R_x = R_y = S_x = S_y = 0$, $Q = 0$, $M = 0$ and $Le = 10$.

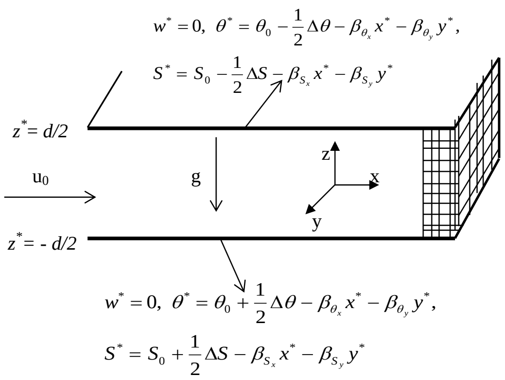

Fig. 1. Schmatic diagram of the physical system.

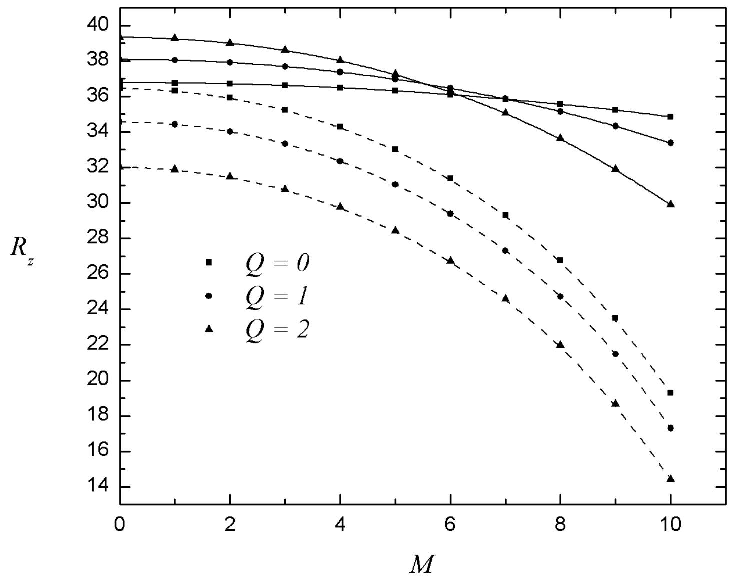

Fig. 2. Variation of R_z with M at $R_x = S_x = 1$ and $S_z = 3$.

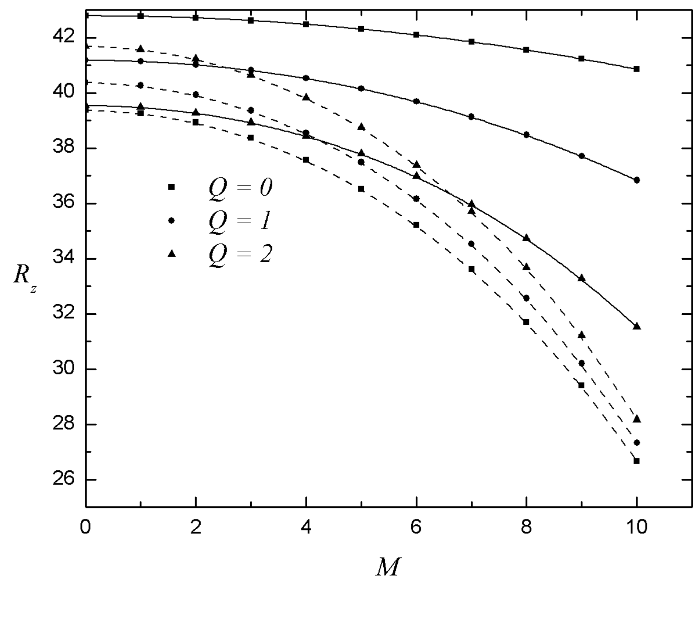

Fig. 3. Variation of R_z with M at $R_x = S_x = 1$ and $S_z = -3$.

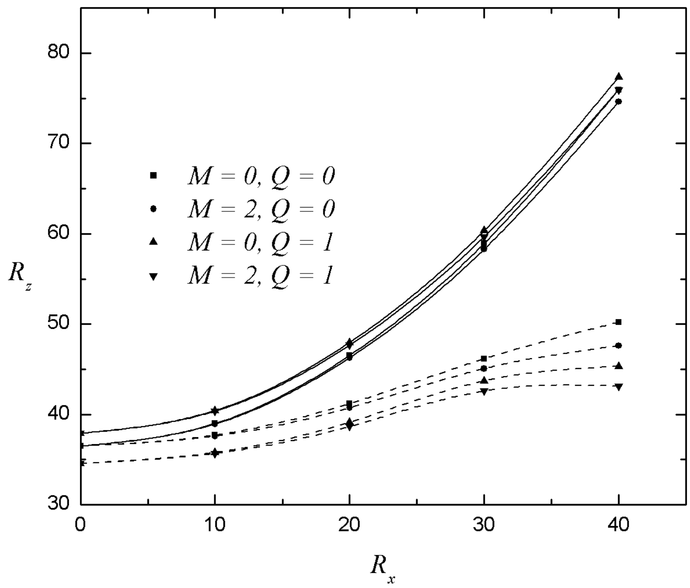

Fig. 4. Variation of R_z with R_x at $Le = 10$ and $S_z = 3$.

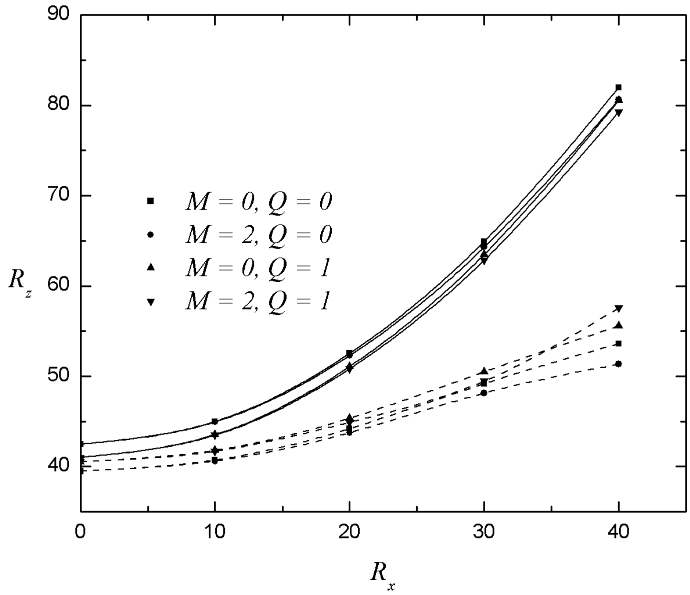

Fig. 5. Variation of R_z with R_x at $Le = 10$ and $S_z = -3$.

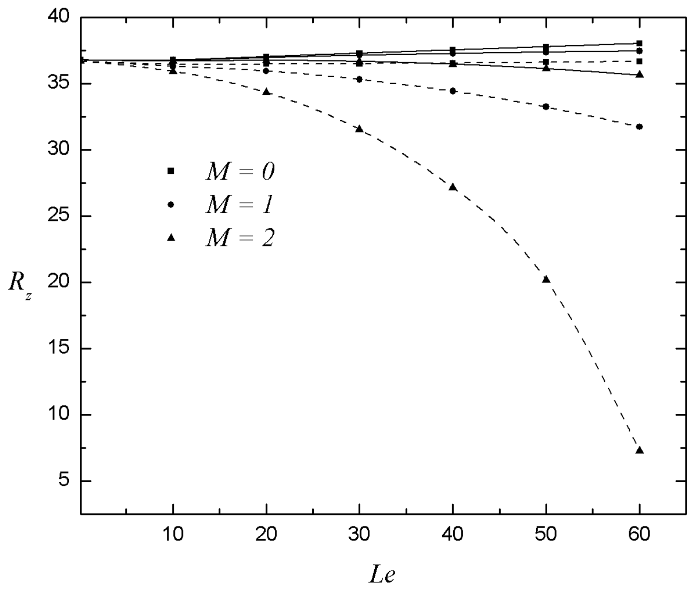

Fig. 6. Variation of R_z with Le at $Q = 0$, $R_x = S_x = 1$ and $S_z = 3$.

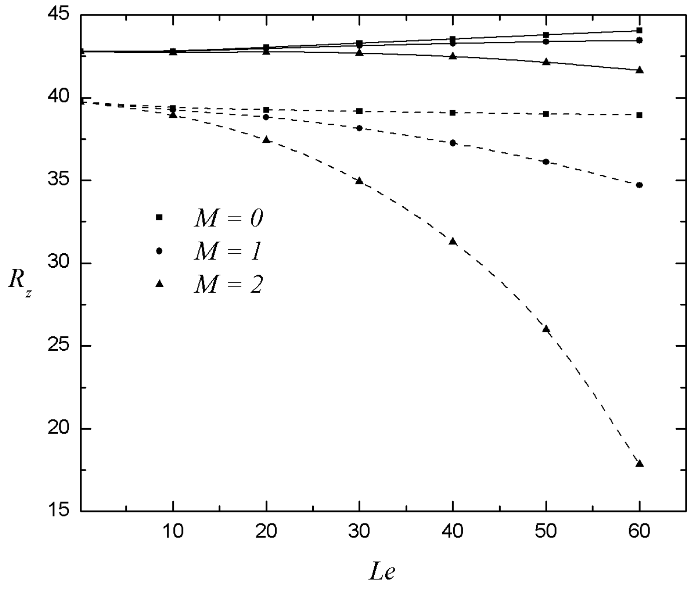

Fig. 7. Variation of R_z with Le at $Q = 0$, $R_x = S_x = 1$ and $S_z = -3$.